Modelling Effects of Sotalol on T-wave Morphology

TP Brennan[1], M Fink[2], D Stokeley[3], B Rodriguez[3], L Tarassenko[1]

[1]Department of Engineering Science, University of Oxford, United Kingdom
[2]Department of Physiology, University of Oxford, United Kingdom
[3]Computing Laboratory, University of Oxford, United Kingdom

Abstract

The QT interval has well-documented shortcomings as a predictor of Torsades de Pointes (TdP) and recent studies have shown that T-wave morphology might provide insight into drug effects on ventricular repolarisation. In this paper, we investigate the underlying mechanisms of the effects of sotalol, a known anti-arrhythmic drug, on T-wave morphology as seen in the surface electrocardiogram (ECG). Analysis of clinical ECG data from a controlled study shows that sotalol alters T-wave morphology, resulting in particular in a decrease in T-wave amplitude. Our multi-scale modelling approach uses a Markov formulation to represent sotalol's interaction with the rapid delayed rectifier potassium channel current (I_{Kr}), validated using experimental data. The ion channel model is then incorporated into a human ventricular cell model, which is then used in a 1D fibre model with transmural heterogeneities to simulate a pseudo-ECG. The simulation results show sotalol-induced changes in I_{Kr} cause rate and dose-dependent increase in action potential duration (APD) and in transmural APD heterogeneities, which result in a decrease of T-wave amplitude and an increase in T-wave dispersion in the pseudo-ECG signal. Thus, our modelling study is able to explain the ionic mechanisms underlying the main sotalol-induced changes in clinical T-wave morphology.

1. Introduction

Drug-induced arrhythmia is a growing concern for regulatory agencies and has become an area of active research. However, the precise mechanisms underlying drug-induced arrhythmia are not clearly understood. Currently, drug-related effects on cardiac behaviour are quantified as changes in the heart rate corrected QT interval (QTc). However, the QT interval as a predictive indicator has number of drawbacks which affect its sensitivity and specificity [1]. Alternative indicators such as the T-wave alternans and indicators based on T-wave morphology have been proposed as improved biomarkers.

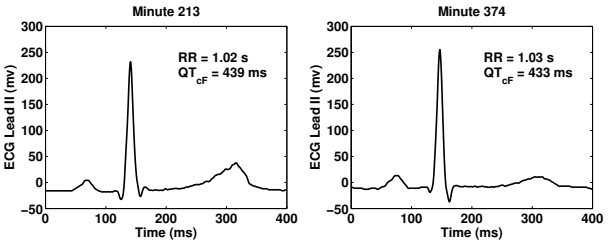

Figure 1. ECG taken Lead II recorded at minute 213 (left) and 374 (right) after oral administration of 320mg dose of sotalol (taken at t=0). The recordings were taken from a 24hr Holter 12-lead surface ECG recording.

Although the origin of the T-wave is not clearly understood, in as much as the relative contributions of transmural versus apex-basal gradients and the role (and existence) of M-cells in human are not known; the T-wave represents cardiac repolarisation of the heterogeneous myocardium [2]. Therefore, alterations in cardiac repolarisation due to drug/ion channel interactions are likely to result in changes in the T-wave morphology but the underlying mechanisms are not well understood.

Sotalol is a class III anti-arrhythmic drug, that is known to inhibit I_{Kr}, thus prolonging QTc by 6.5–11.5% from baseline, and is also known to induce Torsades de Pointes in 5–8% of patients on sustained sotalol treatment [3]. Data deriving from a controlled study (n=6) on sotalol [4] was analysed using a hidden Markov model segmentation algorithm previously developed [5]. QTc increased by 55 ± 7 ms with a maximal QTc change occurring 265 ± 35 min after drug dose. In addition, results showed that sotalol administration resulted in decrease in T-wave amplitude, reaching a minimum 415 ± 32 min after drug administration. Figure 1 highlights the changes observed in T-wave morphology by comparing two ECG waveforms from Lead II taken from minute 213 and minute 374 with comparable RR and QTc intervals.

This study aims to investigate the mechanisms underlying drug-effects on T-wave morphology using a multi-scale model of ventricular electrophysiology. We hypothesise

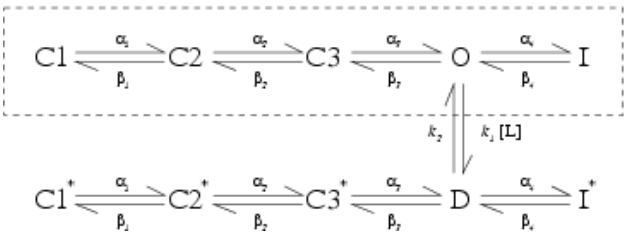

Figure 2. Markov model state diagram of HERG ion channel (I_{Kr})/sotalol interaction. States depicted with an asterisk (*) imply states with sotalol-induced block. C refers to closed state, O to open state, I to inactivated state and D to blocked state.

that prolongation of APD and enhancement of transmural APD heterogeneities caused by sotalol-induced inhibition of I_{Kr} result in a decrease in T-wave amplitude and an increase in QT interval. To test this hypothesis, the interaction of sotalol with I_{Kr} dynamics was modelled using a Markov model formulation. This model was then incorporated into a heterogeneous 1D fibre of human ventricular cells so that changes in T-wave morphology could be simulated for varying drug concentrations.

2. Methods

A 1D fibre model was used, composed of 165 ventricular cells and with a distribution between endocardium, mid-myocardium and epicardium of 50:30:20 [6]. The intercellular conductivity was set to 3 μS [7]. Membrane dynamics were represented by a modified version of the ten Tusscher et al., 2006 model [8] by Fink et al. [9]. The Fink human ventricular model includes improved current formulations for I_{K1} and I_{Kr} as well as alignment of the peak activated currents of I_{K1}, I_{Kr} and I_{Ks} with experimental data. Transmural heterogeneities in ionic currents were incorporated to represent differences observed between endocardial, mid-myocardial and epicardial cells as previously described [10] [8]. In order to simulate the effect of sotalol on cardiac behaviour, a novel continuous-time Markov model of I_{Kr} (see Figure 2) has been developed and validated by our group to model ion channel gating characteristics as well as ligand-binding dynamics [10].

The 1D fibre was paced at its endocardial side at basic cycle length in the range between 400 and 1000ms. The pseudo-ECG or extracellular unipolar potential (Φ_e) generated by the fibre was calculated using the following expression

$$\Phi_e(x', y', z') = \frac{r^2 \sigma_i}{4\sigma_e} \int (-\Delta V_m) \cdot [\Delta \frac{1}{d}] dx \qquad (1)$$

where ΔV_m is the spatial gradient of V_m, σ_i is the intracellular conductivity, σ_e is the extracellular conductiv-

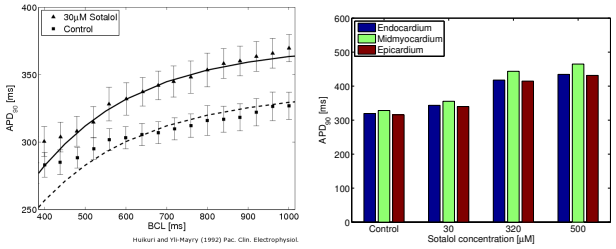

(a) Experimental Data (b) Simulation

Figure 3. Effect of I_{Kr}/sotalol interaction on APD_{90}. **(a)** APD_{90} at several BCL from 400 to 1000 ms. Simulation results are depicted as lines (dashed, control; and solid, with sotalol concentration of 30 μM) and experimental data by Huikuri et al. with symbols (circles, control; and triangles, 30 μM sotalol concetration) **(b)** Simulation of APD_{90} prolongation induced by several sotalol concentrations for endocardial (blue bars), midmyocardial (green bars) and epicardial cells (red bars)

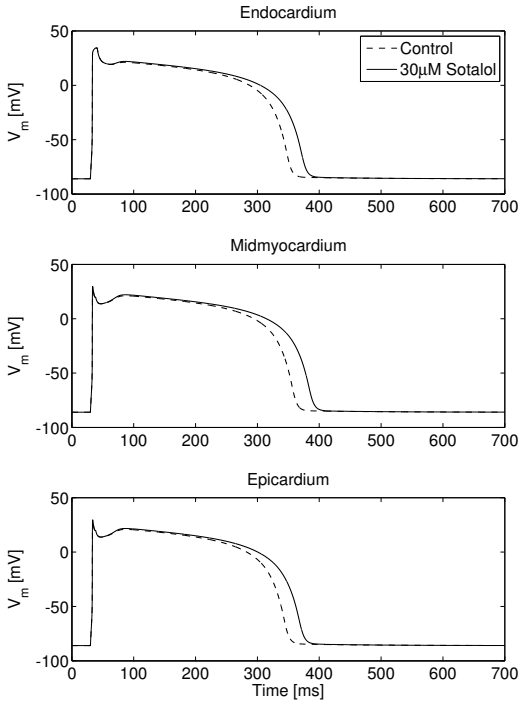

Figure 4. Simulated AP for endocardial, mid-myocardial and epicardial cardiomyocytes under control conditions (dashed lines) and with 30 μM of sotalol (solid lines).

ity, r is the radius of the fibre and d is the euclidean distance from a source point (x, y, z) to the electrode point (x', y', z') [11]. The pseudo-ECG was calculated for an electrode 2 cm from the epicardial edge and excluding 10% of edge cells to remove boundary effects [11]. Conduction Velocity (CV) in control simulations was 45.3 cm.s^{-1}. Computer simulations were run for various sotalol concentrations and changes in QT interval and T-wave morphology were analysed as described in the next section.

3. Results and Discussion

Effect of Sotalol on the Action Potential Duration

Figure 3(a) illustrates the effect of 30 μM of sotalol on APD_{90} at different basic cycle lengths (BCL) obtained in simulations (lines) and experiments (symbols) with human right ventricular tissue from [12]. Both simulation and experimental results show that APD_{90} prolongation by sotalol is rate dependent, which confirms sotalol as a reverse-use dependent drug, i.e. an increased effect at lower heart. Figure 3(b) shows single cell simulation results of the effect of several sotalol concentrations (0-500 μM) on endocardial, midmyocardial and epicardial APD_{90} for a BCL of 1000 ms. Increasing sotalol concentration results in an increase in both APD_{90} and also the APD_{90} differences between endocardial, midmyocardial and epicardial cells. The effect of sotalol on the single cell action potential is further illustrated in Figure 4, which shows the time course of the AP for the three cell types in control and for 30 μM of sotalol, for BCL=1000 ms. The main change is the prolongation of the APD, as also shown and quantified in Figure 3.

Effect of Sotalol on the T-wave morphology

Figure 5 illustrates the effect of several sotalol concentrations (0, 160 and 500 μM) on the pseudo-ECG, as obtained in our simulations using the 1D fibre model. Consistent with our clinical observations, the simulation results show that an increase in drug concentration causes a decrease in T-wave amplitude and an increase in the QTc interval. In particular, 160 μM and 500 μM sotalol resulted in an QTc prolongation of 79 ms and 146 ms respectively.

In order to investigate the causes of sotalol-induced changes in the pseudo-ECG, we quantified changes in APD distribution in the 1D fibre in the presence of varying concentrations of sotalol from 0 to 500 μM. Figure 6 (a) depicts the difference between minimum and maximum APD_{90} measured in the fibre for varying sotalol concentrations. The maximum and minimum APD_{90} measured in the 1D fibre are demarcated by the upper and lower bar limit, respectively. Both maximum and minimum APD_{90}

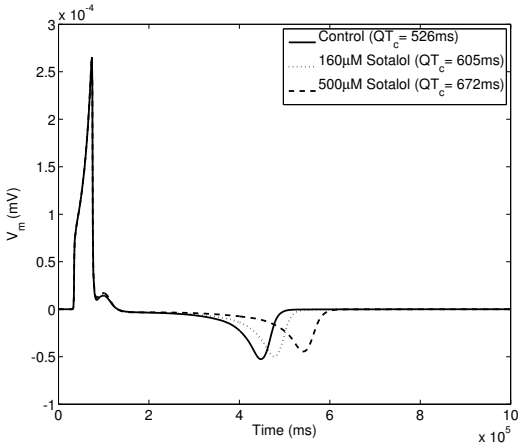

Figure 5. Simulation of the effect of varying concentrations of sotalol on the simulated pseudo-ECG. The 1D fibre was stimulated from its endocardial side with BCL=1000 ms. The QT interval was calculated from time of stimulus application to time at which the pseudo-ECG returned to zero following the T-wave.

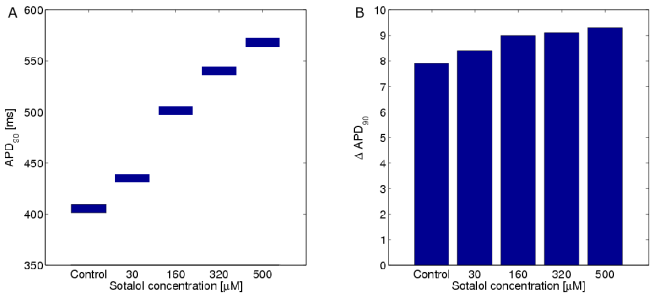

Figure 6. Sotalol-induced changes in transmural heterogeneities in APD_{90}. **(a)** maximum (upper edge) and minimum (lower edge) APD_{90} in 1D fibre for several sotalol concentrations, and **(b)** Δ APD_{90} (i.e. difference between maximum and minimum fibre APD_{90}) for different sotalol concentrations.

increase with increasing drug concentration. Figure 6 (b) highlights sotalol-induced increase in the difference between maximum and minimum fibre APD_{90}. Therefore, the results show that sotalol results in an increase of transmural APD_{90} heterogeneity. Thus, our simulation study shows that prolongation of APD_{90}, and enhancement of transmural APD_{90} heterogeneities caused by the I_{Kr} block by sotalol are responsible for the main changes observed in the simulated pseudo-ECG, namely prolongation of QT interval and changes in T-wave morphology.

Figure 7 illustrates the effect of varying intercellular coupling and I_{Kr} conductance on the simulated pseudo-ECG, in order to assess the sensitivity of our results to variation in these parameters. Varying gap junction resistivity

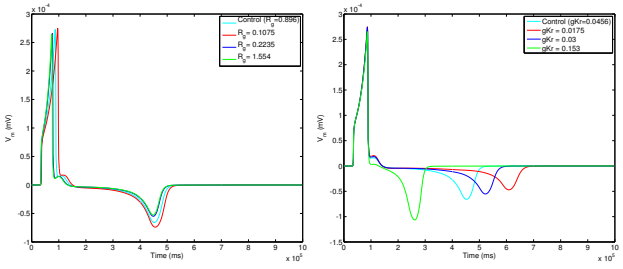

(a)Intercellular coupling (b)I_{Kr} conductance

Figure 7. Sensitivity analysis for different values of **(a)** intercellular coupling and **(b)** conductance of I_{Kr}

from 0.1075 to 1.554 Ω·cm does not effect T-wave morphology significantly, whereas varying g_{Kr} from 0.0175 to 0.153 pA/pF results in both a prolongation of repolarisation and a decrease in T-wave amplitude. The similarity between sotalol effects and the reduction of g_{Kr} is to be expected.

4. Conclusions

This study presents the implementation and validation of a multi-scale model of sotalol-induced effects on ventricular electrophysiology. Clinical effects of sotalol on T-wave morphology and QT interval were replicated in the simulations. Computer simulation results show that inhibition of I_{Kr} by sotalol results in a decrease in T-wave amplitude, prolongation of the APD_{90} and increase in APD_{90} transmural heterogeneities. The effect of sotalol was also seen to be rate and dose dependent. The model limitations need to be considered on the respective levels of implementation. Firstly, the limited data of sotalol interacting with HERG and human I_{Kr} at physiological temperatures reduces the general predictive accuracy of the model. Secondly, the 1D fibre model's structure limits it to in considering only transmural heterogeneities and 1D inter-cellular coupling which is a significant simplification of cardiac electrophysiology. Lastly, the model was simulated using constant pacing rates and the effect of dynamic changes in heart rate were not investigated. Despite these limitations, our study provides significant mechanistic insight into changes in the ECG caused by sotalol interaction with ventricular electrophysiology.

Acknowledgements

This work was supported by a Rhodes Scholarship (to TPB), a Life Science Interface Doctoral Training Centre Studentship (to DS), a Medical Research Council Career Development Award (to BR), the EPSRC-funded Integrative Biology e-science pilot project and the EU BioSim Consortium (MF and BR).

References

[1] Fenichel RR, Malik M, et al. Drug-induced Torsades de Pointes and implications for drug development. J Cardiovas Electrophsiol 2004;15:475–495.

[2] Kootsey JM, Johnson EA. The origin of the T-wave. Crit Rev Bioeng 1980;4(3):223–270.

[3] Fitton A, Sorkin EM. Sotalol: an updated review of it pharmacological properties and therapeutic use in cardiac arrhythmia. Drugs 1993;46(4):678–719.

[4] Sarapa N, Morganroth J, et al. Electrocardiographic identification of drug-induced QT prolongation: assessment by differnet recording and measuring methods. Ann of Noninv Electrocardio 2004;9(1):48–57.

[5] Hughes NP, Tarassenko L. Automated QT interval analysis with confidence measures. In Proceedings of Computers in Cardiology. 2004; .

[6] Drouin E, Charpentier F, et al. Electrophysiologic characteristics of cells spanning the left ventricular wall of human heart: evidence for presence of M cells. J Am Coll Cardiol 1995;26(1):185–192.

[7] Conrath C, Wilders R, et al. Intercellular coupling through gap junctions masks M cells in the human heart. Cardiovasc Res 2004;62:407–414.

[8] Ten Tusccher K, Panfilov A. Alternans and spiral breakup in human ventricular tissue model. Am J Physiol Heart Circ Physiol 2006;291:H1088–H1100.

[9] Fink M, Noble D, et al. Contributions of HERG K^+ current to repolarization of the human ventricular action potential. Phil Trans A Math Phys Eng Sci 2006;364(1842):1207–22.

[10] Brennan T, Fink M, Rodriguez B, Tarassenko L. Modelling effects of Sotalol on action potential morphology using a novel Markov model of HERG channel. In Mediterranean Conference on Medical and Biological Engineering and Computing. In press; .

[11] Gima K, Rudy Y. Ionic current basis of electrocardiographic waveforms: a model study. Circ Res 2002;90:889–896.

[12] Huikuri HV, Yli-Mäyry. Frequency dependent effects of d-sotalol and amiodarone on the action potential duration of the human right ventricle. Pacing Clin Electrophysiol 1992; 15:2103–2107.

Address for correspondence:

Thomas Brennan
Department of Engineering Science
Parks Road, Oxford, OX1 3PJ, United Kingdom
thomas@robots.ox.ac.uk